Three-Dimensional Numerical Simulations of Pulsatile Blood Flow in the Mouse Aortic Arch around Atherosclerotic Plaques

J.P. Hough[1], P. Assemat[1], K.K. Siu[2,3], J.A. Armitage[4], K.G. Contreras[1], A. Aprico[5], K. Andrews[5], A. Dart[5], J. Chin-Dusting[5] and K. Hourigan[1]

[1]Department of Mechanical and Aerospace Engineering & Division of Biological Engineering, Monash University, Victoria 3800, Australia

[2]Monash Biomedical Imaging, Monash University, Victoria 3800, Australia

[3]Australian Synchrotron, 800 Blackburn Rd, Clayton, Victoria 3168, Australia

[4]Department of Anatomy and Developmental Biology, Monash University, Victoria 3800, Australia

[5]Baker IDI Heart and Diabetes Institute, 75 Commercial Rd, Melbourne, Victoria 3004, Australia

Abstract

Atherosclerotic plaques develop at particular sites in the arterial tree, and this regional localisation depends largely on hemodynamic parameters (such as wall shear stress; WSS) as described in the literature. Plaque rupture can result in heart attack or stroke and hence understanding the development and vulnerability of atherosclerotic plaques is critically important. The purpose of this study is to characterise the hemodynamics of blood flow in the mouse aortic arch using numerical modelling. The geometries are digitalised from synchrotron imaging and realistic pulsatile blood flow is considered. In addition, this project seeks to validate a numerical approach that is adaptable to fluid structure interaction methods. Two cases are considered; arteries with and without plaque. The time-averaged WSS distribution in the absence of plaque is qualitatively similar to other results presented in the literature. The presence of plaque was shown to alter the blood flow and hence WSS distribution, with regions of localised high WSS on the wall of the brachiocephalic artery where luminal narrowing is most pronounced.

Introduction

Atherosclerosis is an inflammatory disease of the arterial wall involving lipid deposition and oxidation, leukocyte infiltration, smooth muscle cell migration and extracellular matrix production [3,15]. The lipids form the core of the atherosclerotic plaque, whilst the smooth muscle cells and extracellular matrix produce an overlying fibrous cap.

Plaques develop at particular sites in the arterial tree and it is widely accepted that this localisation is driven by hemodynamic features. In particular, plaques are found on the inner curvatures of arteries characterised by low wall shear stress (WSS) (uni-directional WSS with a low time average) and near bifurcations where oscillatory WSS (bi-directional WSS with a low time average) has been observed [4].

Regions of low WSS have been found to be associated with atherosclerosis development in numerous *in vivo* and numerical studies [7,10,17]. Low WSS has also been linked with biological changes that contribute to plaque growth including up-regulation of adhesion molecules that attract leukocytes, and growth factors that promote the migration and proliferation of smooth muscle cells [3]. Other hemodynamic parameters also play a role, with a laser Doppler volcimetry study revealing atherosclerosis development is enhanced in regions of oscillatory WSS [12]. Numerical simulations also correlate high oscillatory shear index (OSI) with regions prone to atherosclerosis development [10]. However a recent numerical study claims plaque formation does not uniquely associate with low or oscillatory WSS [20]. Several studies suggest a possible role of wall shear stress gradient (WSSG) in atherosclerosis development [5,13]. Therefore whilst atherosclerosis development is associated with disturbed flow, the exact contributions of various hemodynamic features are still under debate.

As plaques develop, they may cause luminal narrowing, leading to a reduction in vessel volume, or undergo expansive remodelling to maintain lumen diameter [17]. Computational fluid studies suggest plaques can alter the pressure and velocity gradients, and this may contribute to plaque progression and vulnerability [2]. Since most computational studies have been conducted in healthy arteries, the influence of plaque on blood flow requires further investigation.

Rupture of the fibrous cap can induce thrombus formation on the plaque surface and can result in myocardial infarction or stroke. Plaque vulnerability depends on the fibrous cap thickness [1], in addition to luminal remodelling and blood hemodynamics. Regions of high WSS may be associated with plaque rupture [8]. However, structural stresses are thought to play a more dominant role, being several orders of magnitude higher than the WSS induced by blood flow [16]. Tang et al. [18] associated fibrous cap disruption with regions of high structural stresses, whilst other studies have identified high principal stresses on the shoulder regions of the fibrous cap [11]. Most biomechanical models of plaque vulnerability are based on the theory that plaque rupture will occur when the tissue stress reaches a threshold [16].

The purpose of this study is to investigate the hemodynamics of blood flow through the mouse aortic arch with and without plaques. The focus is to improve understanding of plaque development and vulnerability in realistic geometry and provide insight into the influence of plaque on hemodynamics. Furthermore, this paper seeks to validate a numerical approach that is adaptable to the implementation of fluid structure interaction (FSI) methods.

Model Description

Animal Preparation

An Apolipoprotein E knockout (ApoE-/-) mouse model was used as a model of spontaneous atherosclerosis development. Wild type C57/B6 mice were used as controls since mice do not

naturally develop atherosclerosis. Mice were fed with a high fat diet (21% fat; 0.15% cholesterol). Adult mice were given a terminal dose of anaesthetic and blood was cleared from the vasculature by transcardial perfusion with heparinised saline. Karnofsky's fluid (2% glutaraldehyde + 4% paraformaldehyde in 0.1M phosphate buffer, pH 7.4) was then used to perfusion fix the tissue, preserving vessel morphology. Following dissection and dehydration through graded butanol, the tissues were embedded in paraffin

Vessel Geometry

The mice aortas were imaged by micro-computed tomography (μ-CT). This employs 15keV monochromatic synchrotron X-rays (PSI, Swiss Light Source synchrotron, Switzerland) that are detected by a CCD detector. The μ-CT data was reconstructed into two-dimensional (2D) vessel slices using the program X-TRACT developed at the CSIRO [9] (http://www.ts-imaging.net/Services/_AppInfo/X-TRACT.aspx), which employs the Paganin algorithm [14]. Image reconstruction and segmentation of the vessel wall, plaque and lumen was conducted in the software AVIZO (figure 1). The geometry was compared with histological data (obtained by staining 5μm cross sections of the aorta with Masson's Trichrome) to verify plaques were well defined. The vessel lumen (fluid compartment) was imported into ICEM CFD, where the ends of the vessel were extended to ensure flow is fully developed at the vessel outlets.
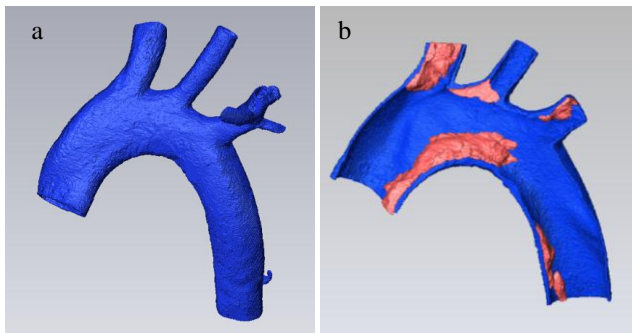

Figure 1: (a) Reconstructed mouse aortic arch. (b) Half of the mouse aortic arch revealing the atherosclerotic plaque (red) on the vessel wall (blue).

Mesh

Meshing was conducted in the program ICEM CFD. A structured hexahedral mesh was produced using blocking and O-grid techniques. These techniques allow the mesh density to be tightly controlled, including the number and size of boundary layers, in addition to node distribution along the surface (figure 2). A structured approach will be crucial in future FSI simulations to ensure the convergence of the FSI methods (parallel work, not presented here, has been undertaken to check the convergence of FSI methods in a model of straight vessel).

Boundary Conditions

The imposed boundary conditions in computational fluid dynamics (CFD) simulations have a significant influence on the numerical results, and thus accurately defining the boundary conditions is crucial. Velocity waveforms are frequently used as inlet boundary conditions, using scaling techniques to obtain realistic waveforms from measurements in unconscious animals [10,20]. Pressure profiles have also been employed as inlet conditions in a numerical study of the human aortic arch [21]. Outlet boundary conditions are commonly defined as a percentage of the inlet flow rate [6,20]; however, this assumes the flow distribution remains constant throughout the cardiac cycle. In this study, boundary conditions at the inlets and outlets will be defined based on redistributed oscillating volumetric flow

rates, as described by Trachet et al. [19]. These flow rates are based on ultrasound measurements at the inlets and outlets that are redistributed to satisfy on the rigid wall assumption. This approach is thought to be more accurate than the use of percentage flow rates. Fourier series was used to obtain equations of the flow rates from the data in Trachet et al. [19] (figure 3). A heart rate of 600 beats per minute was assumed. Walls were modelled as rigid with a no slip boundary condition.
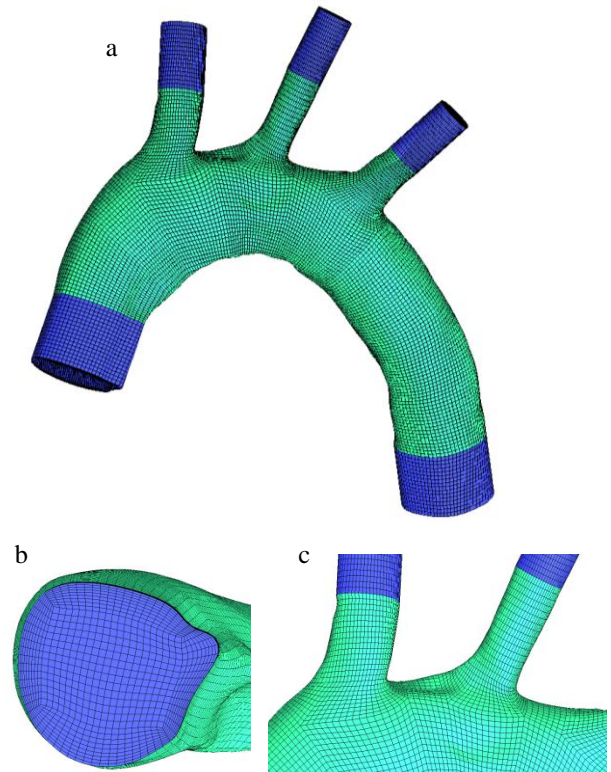

Figure 2: (a) Hexahedral mesh for aortic arch with plaque. (b) Close up of mesh at inlet showing boundary layers generated by O-grid. (c) Close-up of mesh at branch points. In each image, the green colour corresponds to the geometry obtained by μ-CT and the blue corresponds to the extensions.
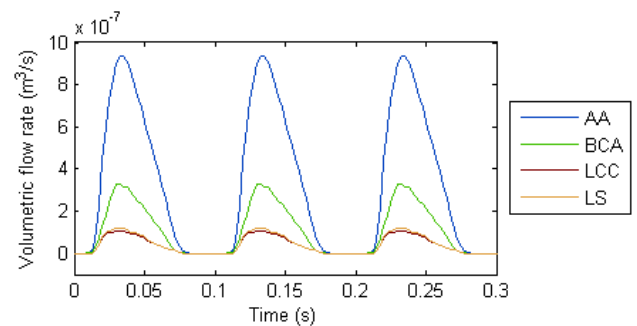

Figure 3: Oscillatory volumetric flow rates for the ascending aorta (AA), brachiocephalic artery (BCA), left common carotid artery (LCC) and left subclavian artery (LS) used as boundary conditions. Reconstructed from Trachet et al. [19].

CFD Simulations

Numerical modelling was performed in ANSYS CFX. The Navier-Stokes equations were solved using the element based finite volume methods. Blood was considered Newtonian, with a density and dynamic viscosity of $1060kg/m^3$ and 0.004Pa.s, respectively [6,19]. The calculation of the time evolution of the solution was conducted for three cycles (0.3s), with a timestep of 0.001s.

Results

The time-averaged WSS distribution for vessel without plaque is presented in figure 4. The figure demonstrates a region of low WSS on the inner curvature of the aortic arch, where plaque formation is characteristically observed. There is also a noticeable region of local high WSS on the downstream surface of the brachiocephalic artery (BCA). This WSS distribution is qualitatively similar to the results presented in Trachet et al. [19]. The order of magnitude obtained in this study is also similar to that presented in Trachet et al. [19]; however the WSS values are slightly larger for the present study (maximum time-averaged WSS for the present study is 10Pa, whilst maximum time-averaged WSS in Trachet et al. [19] is 8Pa). This can be explained by the difference in geometry dimensions; on average the branch diameters of the geometry used in Trachet et al. [19] are 1.3 times larger than the diameters corresponding to vessel without plaque used in the present study. In addition, the local regions of high WSS on the downstream sides of the first two branches (shown by arrows in Figure 4) are qualitatively similar to those presented in Huo et al. [10].
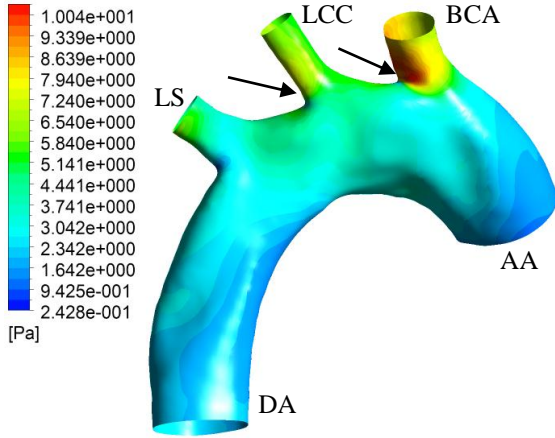

Figure 4: Time average WSS distribution on the artery wall for vessel without plaque. The arrows indicate regions of local high WSS on the downstream side of the first two branches.

Diameter (mm)	AA	BCA	LCC	LS	DA
Vessel without plaque	1.0	0.55	0.37	0.41	0.87
Vessel with plaque	0.98	0.45	0.37	0.38	0.86

Table 1: Equivalent diameters of the ascending aorta (AA), brachiocephalic artery (BCA), left common carotid artery (LCC), left subclavian artery (LS) and descending aorta (DA). The diameters were measured at the end of each branch for vessels with and without plaque.

The presence of plaque was found to alter the time-averaged WSS distribution on the vessel wall (Figure 5). In particular, there is a region of low WSS on the downstream side of the main aortic plaque, indicated by an arrow in the figure. This region of low WSS could contribute to plaque progression, leading to enlargement of the existing atherosclerotic plaque. In addition, the magnitude of the highest WSS is increased significantly, and the position of local high WSS is altered. The plaque causes significant narrowing of the brachiocephalic artery, as shown by the vessel cross section in figure 1(b) and the branch diameters for vessel with and without plaque in table 1.The high WSS is located on the upstream face of the brachiocephalic artery, corresponding to the site of maximal luminal narrowing. The WSS distribution on the brachiocephalic branch at different stages throughout the cardiac cycle is shown in figure 5. This highlights the variation in WSS that occurs throughout the cardiac cycle, in addition to the variation induced by the presence of the plaque.
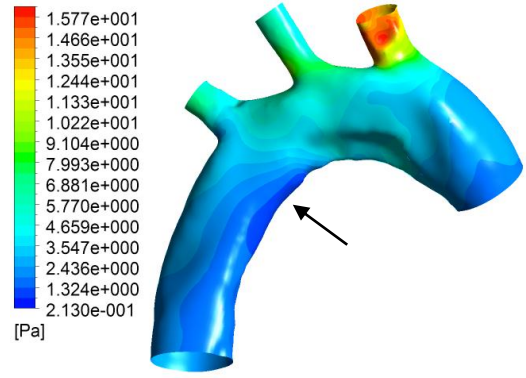

Figure 5: Time average WSS distribution on the artery wall for vessel with plaque. The arrow indicates a region of low WSS on the downstream side of the main aortic plaque.

Several studies suggest plaque rupture may be associated with high WSS [8,18], and hence the local maximum of WSS on the surface of the brachiocephalic plaque could contribute to plaque rupture. Furthermore, it has been proposed by Vengrenyuk et al. [22] that the brachiocephalic plaque resembles human vulnerable plaque, whilst plaques on the aortic arch resemble stable lesions. However, these findings were based on studies of peak and circumferential stress rather than WSS. It is likely that structural stresses are a more important indicator for predicting plaque rupture [16]. Such structural stresses will be investigated in future FSI simulations.
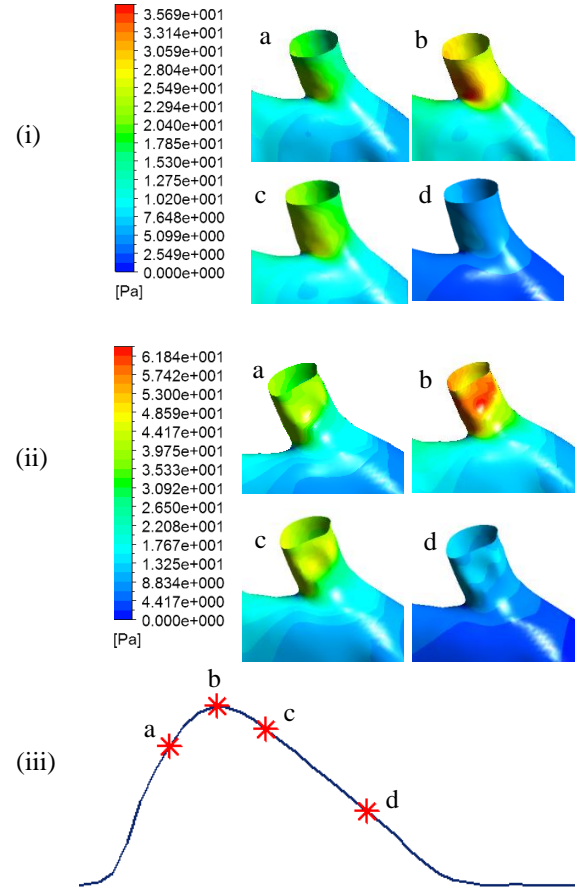

Figure 6: WSS distribution on the brachiocephalic artery at four stages during the cardiac cycle as indicated on the volumetric flow rate diagram (iii); (a) systolic acceleration, (b) peak systole and (c & d) systolic deceleration. The vessel without plaque is presented above (i), and the vessel with plaque in the lower part of the figure (ii).

Conclusions

Given the limited numerical data on blood hemodynamics in the presence of atherosclerosis, the main goal of this study was to develop methods for modelling pulsatile blood flow in an artery with plaque. The WSS results in the absence of plaque are qualitatively similar to those presented in the literature. The presence of plaque was found to increase WSS significantly, particularly in regions with large luminal narrowing, such as the brachiocephalic artery. The local change in flow observed due to the presence of the plaque could have a large impact on the structural behaviour when deformable walls are taken into account in future FSI simulations.

Acknowledgments

References

[1] Avgerinos, E.D., Giannakopoulos, T.G., Kadoglou, N.P., Liapis, C.D., Moulakakis, K.G. & Papapetrou, A., Biomarkers for Diagnosis of the Vulnerable Atherosclerotic Plaque, *Interventional Cardiology*, **3**(2), 2011, 223.

[2] Chaichana, T., Sun, Z. & Jewkes, J., Computational Fluid Dynamics Analysis of the Effect of Plaques on the Left Coronary Artery, *Comput. Math. Method M.*, **2012**, 2012, pp 9.

[3] Chatzizisis, Y.S., Coskun, A.U., Jonas, M., Edelman, E.R., Feldman, C.L. & Stone, P.H., Role of Endothelial Shear Stress in the Natural History of Coronary Atherosclerosis and Vascular Remodelling: Molecular, Cellular and Vascular Behaviour. *J. Am. Coll. Cardiol.,* **49**(25), 2007, 2379-2393

[4] Cheng, C., Tempel, D., Van Haperen, R., Van Der Bann, A., Grosveld, F., Daemen, M.J., Krams, R. & De Crom, R., Atherosclerotic Lesion Size and Vulnerability are Determined by Patterns of Fluid Shear Stress, *J. Am. Heart Assoc.*, **113**, 2006, 2744-2753.

[5] DePaola, N., Gimborne, M.A., Davis, J.F. & Dewey, F., Vascular Endothelium Responds to Fluid Shear Stress Gradients, *Atherosclerosis and Thrombosis*, **12**, 1991, 1254-1257.

[6] Feintuch, A., Ruengsakulrach, P., Lin, A., Zhang, J., Zhou, Y.Q., Bishop, J., Davidson, L., Courtman, D., Foster, F.S., Steinman, D.A., Henkelman, R.M. & Ethier, C.R., Hemodynamics in the Mouse Aortic Arch as Assessed by MRI, Ultrasound, and Numerical Modeling, *Am. J. Physiol. Heart Circ. Physiol.*, **292**, 2007, H884-H892.

[7] Gibson, C.M., Diaz, L., Kandarpa, K., Sacks, F.M., Pasternak, R.C., Sandor, T., Feldman, C. & Stone, P.H., Relation of Vessel Wall Shear Stress to Atherosclerosis Progression in Human Coronary Arteries, *J. Am. Heart Assoc.*, **13**, 1993, 210-315.

[8] Groen, H.C., Gijsen, F.J.H., van der Lugt, A., Hatsukami, T.S., van der Steen, A.F.W., Yuan, C. & Wentzel, J.J., Plaque Rupture in the Carotid Artery is Localized at the High Shear Stress Region, *Stroke,* **38**, 2007, 2379-2381.

[9] Gureyev, T.E., Nesterets, Y., Ternovski, D., Thompson, D., Wilkins, S.W., Stevenson, A.W., Sakellariou, A. & Taylor, J.A., Toolbox for Advanced X-ray Image Processing, *Proc SPIE,* **8141**, 2011, 81410B-14.

[10] Huo, Y., Guo, X. & Kassab, G.S., The Flow Field along the Entire Length of the Mouse Aorta and Primary Branches, *Ann. Biomed. Eng.*, **36**(5), 2008, 685-699.

[11] Kock, S.A., Nygaard, J.V., Eldrup, N., Frund, E.T., Klaerke, A., Paasake, W.P., Erling, F. & Kim, W.Y., Mechanical Stresses in Carotid Plaques Using MRI-based Fluid-Structure Interaction Models, *J. Biomech.,* **41**, 2008, 1651-1658.

[12] Ku, D.N., Giddens, D.P., Zarins, C.K. & Glagov, S., Pulsatile Flow and Atherosclerosis in the Human Carotid Bifurcation, *J. Am. Heart Assoc.*, 5, 1985, 293-302.

[13] Lei, M., Kleinstreuer, C. & Truskey, G.A., Numerical Investigation and Prediction of Atherogenic Sites in Branching Arteries, *J. Biomech. Eng.*, **117**(3), 1995, 350-357.

[14] Paganin, D., Mayo, S.C., Gureyev, T.E., Miller, P.R. & Wilkins S.W., Simultaneous Phase and Amplitude Extraction from a Single Defocused Image of a Homogeneous Object, *J. Microscopy*, **206**, 2002, 33-40.

[15] Pello, O.M., Silvestre, C., Pizzol, M.D. & Andres, V., A Glimpse of the Phenomenon of Macrophage Polarisation During Atherosclerosis, *Immunobiology*, **216**, 2011, 1172-1176.

[16] Sadat, U., Teng, Z. & Gillard J.H., Biomechanical Structural Stresses of Atherosclerotic plaques, *Expert Review of Cardiovascular Therapy,* **8**(10), 2010, 1469-1481.

[17] Stone, P.H., Coskun, A.U., Kinlay, S., Popma, J.J., Sonka, M., Wahle, A., Yeghiazarians, Y., Maynard, C., Kuntz, R.E. & Feldman, C.L., Regions of Low Endothelial Shear Stress are the Sites where Coronary Plaque Progresses and Vascular Remodelling Occurs in Humans: an in Vivo Serial Study, *Eur. Heart J.*, **28**, 2007, 705-710.

[18] Tang, D., Teng, Z., Canton, G., Yang, C., Ferguson, M., Huang, X., Zheng, J., Woodard, P.K. & Yuan, C., Sites of Rupture in Human Atherosclerotic Carotid Plaques are Associated with High Structural Stresses: An In Vivo MRI-Based 3D Fluid-Structure Interaction Study, *Stroke,* **40**, 2009, 3258-3263.

[19] Trachet, B., Bols, J., De Santis, G., Vandenberghe, S., Loeys, B. & Segers, P., The Impact of Simplified Boundary Conditions and Aortic Arch Inclusion on CFD Simulations in the Mouse Aorta: A Comparison with Mouse-Specific Reference Data, *J. Biomech. Eng.*, **133**, 2011, 1-13.

[20] Van Doormaal, M.A., Kazakidi, A., Wylezinska, M., Hunt, A., Tremoleda, J.L., Protti, A., Bohraus, Y., Gsell, W., Weinberg, P.D. & Ethier, C.R., Haemodynamics in the Mouse Aortic Arch Computed from MRI-Derived Velocities at the Aortic Root, *J. R. Soc. Interface*, (EPub) 2012, 1-11.

[21] Vasava, P., Jalali, P., Dabagh, M. & Kolari, P.J., Finite Element Modelling of Pulsatile Blood Flow in Idealized Model of Human Aortic Arch: Study of Hypotension and Hypertension. *Comput. Math. Method M.*, **2012**, 2012, 1-14.

[22] Vengrenyuk, Y., Kaplan, T.J., Cardoso, L., Randolph, G.J. & Weinbaum, S., Computational Stress Analysis of Atherosclerotic Plaques in ApoE Knockout Mice. *Ann. Biomed. Eng.,* **38**(3), 2010, 738-74